BBM 418 - Computer Vision Laboratory

Assignment 1 Report

Ahmet İkbal Kayapınar
2210356043

Methods

Hough Transform

The Hough Transform is a powerful technique for detecting straight lines in a binary edge image by mapping points from the image space to a parameter space. It works by representing lines in polar coordinates using the equation $\rho = x\cos\theta + y\sin\theta$, where ρ is the perpendicular distance from the origin to the line, and θ is the angle between the x-axis and the line's normal. By iterating over a set of predefined angles and calculating the corresponding ρ for each edge point, the transform accumulates votes in a matrix called the accumulator. Peaks in the accumulator correspond to prominent lines in the original image. To enhance robustness, a thresholding process filters out weak detections, and non-maximum suppression ensures that only the most significant lines are detected by comparing each candidate to its local neighborhood. This process allows reliable detection of lines regardless of their position or orientation within the image.

RANSAC

RANSAC (Random Sample Consensus) is a robust iterative algorithm designed to fit a model to data contaminated with outliers. It operates by repeatedly selecting random subsets of the input data and using these subsets to estimate model parameters. For line fitting, this involves randomly picking two distinct points and computing the line passing through them using the slope-intercept form $y = mx + c$. For each iteration, the model is evaluated against the entire dataset by calculating the perpendicular distances of all points to the estimated line. Points whose distances fall below a predefined threshold are considered inliers. The quality of a model is determined by the number of inliers it attracts, with ties broken by considering the model's overall error. After a fixed number of iterations, the best model is selected based on the largest consensus set of inliers. This approach allows RANSAC to effectively fit a line to data even when a substantial portion of the points are outliers, as only the points supporting a valid model contribute to its evaluation.

Quadrilateral Detection

The most challenging and fundamental problem of the assignment was detecting the rectangles of the papers using the lines found. I experimented a lot with multiple ideas for this part. Before explaining the main solution method, I will discuss the two methods I tried before and why I chose the current solution method instead.

1) Initially, considering that the Hough Transform algorithm finds too many lines in some images, I thought about filtering these lines using RANSAC. For this, I fed the input of the points on the detected lines to RANSAC. To simplify the geometric transformation part, I classified the lines detected by the Hough Transform as horizontal and vertical, and I experimented with having RANSAC select two lines from each class. This way, the most distinct rectangle that passed through two filtering stages would automatically emerge. However, I abandoned this idea due to reasons such as the Hough Transform failing to detect sufficient lines in some images, the line selection process by RANSAC not being applicable as theoretically intended, and the method working incorrectly in practice.

2) After giving up on filtering lines using RANSAC, I applied a method where I added the lines detected by RANSAC to the lines found by the Hough Transform for images where the Hough Transform was insufficient. To find the appropriate rectangle, I tried finding all line intersections on the image and selecting the largest rectangle among them. Although this method was much more workable and generalizable compared to the previous one, I still found it lacking. First of all, the processing times were much longer than I expected, and processing some images could take up to half a minute. Additionally, when too many lines were detected, it would select corners from irrelevant parts of the image and form rectangles unrelated to the paper. While this didn't severely damage the image and thus didn't reduce the SSIM score significantly, it meant that the image was almost entirely unprocessed, failing to achieve the intended result.

Main Solution: To address the shortcomings of the previous methods, I used a different approach. Like in the second solution, I added the lines detected by RANSAC to those found by the Hough Transform. Instead of focusing

only on the corners, I grouped the lines according to a certain angle tolerance and found lines perpendicular to each other within that tolerance. In this way, I solved the problem of selecting unrelated corners. Among the rectangles formed by perpendicular lines, I ultimately chose the one with the largest area and applied the geometric transformation.

Geometric Transformation

Geometric transformation using homography involves mapping points from one plane to another through a projective transformation, which can handle translation, rotation, scaling, and perspective distortion. To determine the transformation, a homography matrix H is computed using a set of corresponding points between the source and destination planes. This matrix is obtained by solving a linear system derived from the relationship between the points, resulting in an 3×3 matrix that maps any point (x, y) in the source image to a point (u, v) in the destination image.

Once the homography matrix is calculated, image warping is performed through bilinear interpolation. The transformation is applied by finding the inverse mapping for every pixel in the output image, determining where it originated from in the source image. Since these mapped points do not generally fall exactly on pixel coordinates, the intensity value at each point is obtained by interpolating the values of the four nearest pixels. This bilinear interpolation ensures smooth and accurate mapping even when scaling or rotating the image. By reconstructing the output image using these interpolated values, the process effectively applies the geometric transformation defined by the homography matrix.

Examples

Here are correct and incorrect examples for each class:

Image 1

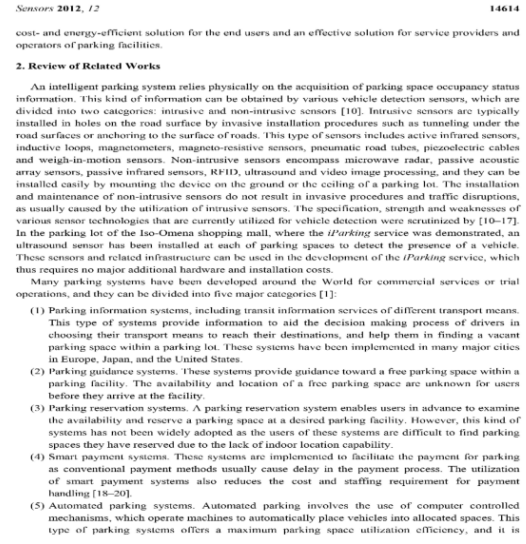

Sensors **2012**, *12* **14614**

cost- and energy-efficient solution for the end users and an effective solution for service providers and operators of parking facilities.

2. Review of Related Works

An intelligent parking system relies physically on the acquisition of parking space occupancy status information. This kind of information can be obtained by various vehicle detection sensors, which are divided into two categories: intrusive and non-intrusive sensors [10]. Intrusive sensors are typically installed in holes on the road surface by invasive installation procedures such as tunneling under the road surfaces or anchoring to the surface of roads. This type of sensors includes active infrared sensors, inductive loops, magnetometers, magneto-resistive sensors, pneumatic road tubes, piezoelectric cables and weigh-in-motion sensors. Non-intrusive sensors encompass microwave radar, passive acoustic array sensors, passive infrared sensors, RFID, ultrasound and video image processing, and they can be installed easily by mounting the device on the ground or the ceiling of a parking lot. The installation and maintenance of non-intrusive sensors do not result in invasive procedures and traffic disruptions, as usually caused by the utilization of intrusive sensors. The specification, strength and weaknesses of various sensor technologies that are currently utilized for vehicle detection were scrutinized by [10–17]. In the parking lot of the Iso-Omena shopping mall, where the *iParking* service was demonstrated, an ultrasound sensor has been installed at each of parking spaces to detect the presence of a vehicle. These sensors and related infrastructure can be used in the development of the *iParking* service, which thus requires no major additional hardware and installation costs.

Many parking systems have been developed around the World for commercial services or trial operations, and they can be divided into five major categories [1]:

(1) Parking information systems, including transit information services of different transport means. This type of systems provide information to aid the decision making process of drivers in choosing their transport means to reach their destinations, and help them in finding a vacant parking space within a parking lot. These systems have been implemented in many major cities in Europe, Japan, and the United States.

(2) Parking guidance systems. These systems provide guidance toward a free parking space within a parking facility. The availability and location of a free parking space are unknown for users before they arrive at the facility.

(3) Parking reservation systems. A parking reservation system enables users in advance to examine the availability and reserve a parking space at a desired parking facility. However, this kind of systems has not been widely adopted as the users of these systems are difficult to find parking spaces they have reserved due to the lack of indoor location capability.

(4) Smart payment systems. These systems are implemented to facilitate the payment for parking as conventional payment methods usually cause delay in the payment process. The utilization of smart payment systems also reduces the cost and staffing requirement for payment handling [18–20].

(5) Automated parking systems. Automated parking involves the use of computer controlled mechanisms, which operate machines to automatically place vehicles into allocated spaces. This type of parking systems offers a maximum parking space utilization efficiency, and it is

Image 2

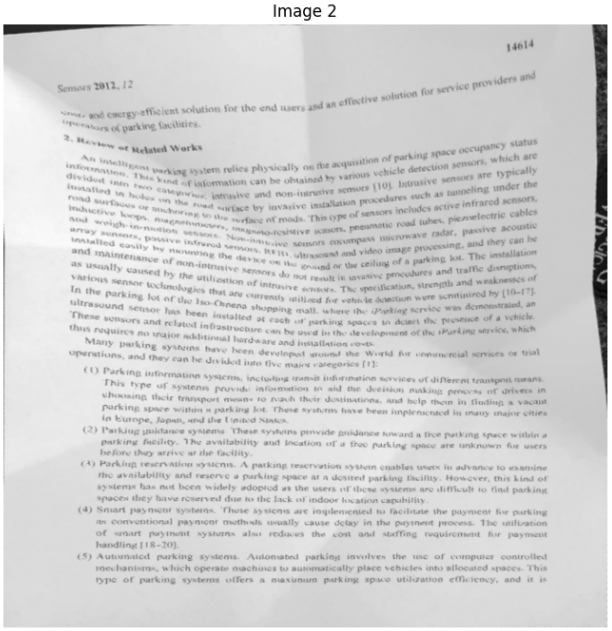

14614

Sensors 2012, 12

cost- and energy-efficient solution for the end users and an effective solution for service providers and operators of parking facilities.

2. Review of Related Works

An intelligent parking system relies physically on the acquisition of parking space occupancy status information. This kind of information can be obtained by various vehicle detection sensors, which are divided into two categories: intrusive and non-intrusive sensors [10]. Intrusive sensors are typically installed in holes on the road surface by invasive installation procedures such as tunneling under the road surfaces or anchoring to the surface of roads. This type of sensors includes active infrared sensors, inductive loops, magnetometers, magneto-resistive sensors, pneumatic road tubes, piezoelectric cables and weigh-in-motion sensors. Non-intrusive sensors encompass microwave radar, passive acoustic array sensors, passive infrared sensors, RFID, ultrasound and video image processing, and they can be installed easily by mounting the device on the ground or the ceiling of a parking lot. The installation and maintenance of non-intrusive sensors do not result in invasive procedures and traffic disruptions, as usually caused by the utilization of intrusive sensors. The specification, strength and weaknesses of various sensor technologies that are currently utilized for vehicle detection were scrutinized by [10–17]. In the parking lot of the Iso-Omena shopping mall, where the *iParking* service was demonstrated, an ultrasound sensor has been installed at each of parking spaces to detect the presence of a vehicle. These sensors and related infrastructure can be used in the development of the *iParking* service, which thus requires no major additional hardware and installation costs.

Many parking systems have been developed around the World for commercial services or trial operations, and they can be divided into five major categories [1]:

(1) Parking information systems, including transit information services of different transport means. This type of systems provide information to aid the decision making process of drivers in choosing their transport means to reach their destinations, and help them in finding a vacant parking space within a parking lot. These systems have been implemented in many major cities in Europe, Japan, and the United States.

(2) Parking guidance systems. These systems provide guidance toward a free parking space within a parking facility. The availability and location of a free parking space are unknown for users before they arrive at the facility.

(3) Parking reservation systems. A parking reservation system enables users in advance to examine the availability and reserve a parking space at a desired parking facility. However, this kind of systems has not been widely adopted as the users of these systems are difficult to find parking spaces they have reserved due to the lack of indoor location capability.

(4) Smart payment systems. These systems are implemented to facilitate the payment for parking as conventional payment methods usually cause delay in the payment process. The utilization of smart payment systems also reduces the cost and staffing requirement for payment handling [18–20].

(5) Automated parking systems. Automated parking involves the use of computer controlled mechanisms, which operate machines to automatically place vehicles into allocated spaces. This type of parking systems offers a maximum parking space utilization efficiency, and it is

Figure 1: Correct Fold Example

Image 1

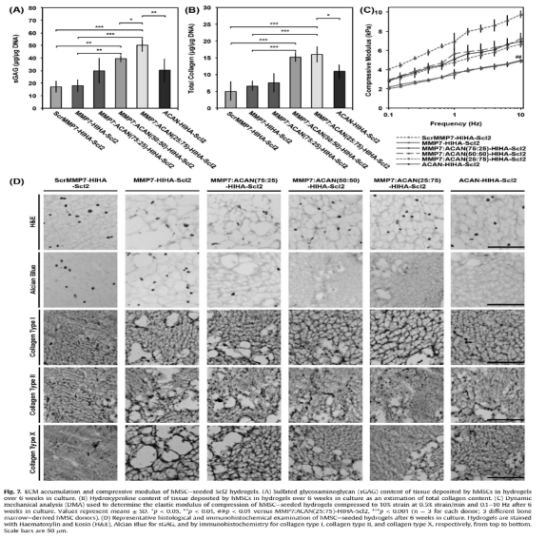

Image 2

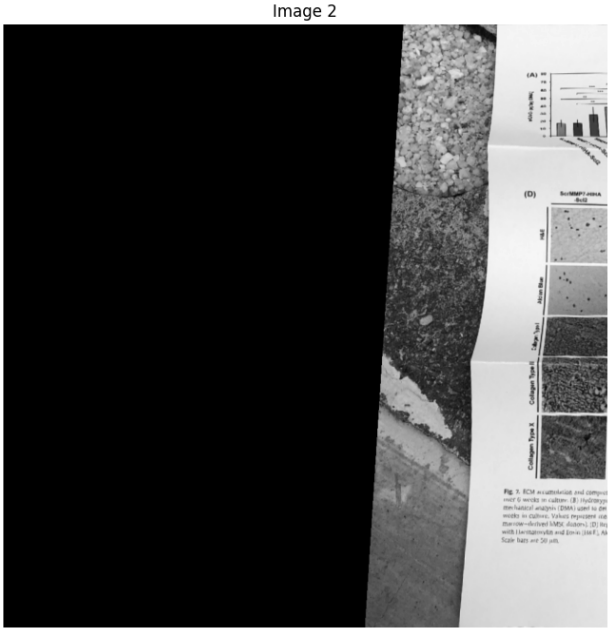

Figure 2: Incorrect Fold Example

Image 1

346 *EG.W. Van Nieuwerburgh et al.*

disorder or patients with a total score of 15 or more on the 17-item HAM-D on admission were excluded. Other exclusion criteria were diagnoses of major depression, bipolar disorder, schizophrenia, other psychotic conditions, substance related disorder within the last 6 months, primary anxiety disorders, personality disorders, use of a concomitant psychotropic drug, organic mental disorders, epilepsy and any structural central nervous system disorder. Furthermore, clinically significant cardiovascular, gastrointestinal, pulmonary, renal, hepatic, endocrine or hematological conditions resulted in exclusion from this study. Of these 91 patients, 17 dropped out of this study because of lack of motivation, uncertain medication use or failure to collect blood for determination of drug plasma concentrations. The 74 remaining patients have following characteristics: 39.2% male; positive family history, 36.1%; age at onset, 19.5 ± 9.0; age at admission to study, 36.3 ± 11.6; baseline YBOCS score, 25.0 ± 5.7.

The patients were randomly assigned in a 12-week, double-blind trial to receive dosages titrated upward to 300 mg/day of venlafaxine or 60 mg/day of paroxetine, using a fixed dosing schedule. (see Denys et al. [4] for details on the dosing schedule). The patients received no additional drugs affecting the P450 enzyme system and were treatment free at baseline for at least 1 month. Primary efficacy was assessed by the change from basecline on the YBOCS, and response was defined as a ≥25% reduction on the YBOCS.

Blood samples were collected from each subject and frozen at −80°C. Blood levels of paroxetine, venlafaxine and *O*-desmethylvenlafaxine were determined at weeks 0, 1, 3, 5, 8, 10 and 12 by high-performance liquid chromatography with fluorescence detection [5]. Blood for the drug level determinations was collected at the response assessment in those weeks, at a random time point after ingestion of the medicine.

DNA was extracted from 10 µl of peripheral blood according to standard procedures. The samples were genotyped using TaqMan® Drug Metabolism Genotyping Assays from Applied Biosystems for the NCBI dbSNP identification numbers rs3892097 (1846G >A polymorphism, resulting in the inactive CYP2D6 allele 4 [6]), rs5030655 (1707T >Del polymorphism, resulting in the inactive CYP2D6 allele 6 [6]), rs1065852 (100C >T polymorphism, resulting in the reduced activity CYP2D6 allele 10 when not in combination with the 1846G >A polymorphism [7]) and rs28371725 (2988G >A polymorphism, resulting in the reduced activity CYP2D6 allele 41 [8]. In a Caucasian population, the frequency of all inactive and all reduced activity alleles is about 35%, of which 80–90% are caused by the four analyzed SNPs [9,10].

Results

The measured minor allele frequencies for rs3892097, rs5030655, rs1065852, and rs28371725 are 0.24, 0.02, 0.26 and 0.08, respectively. This is in accordance with the minor allele frequencies reported by Applied Biosystems: 0.20, 0.00, 0.21 and 0.11, respectively. Fifty-seven percent of the patients have at least one reduced activity CYP2D6 allele while 13% have two reduced activity CYP2D6 alleles.

To assess the effect of the polymorphisms on the medication plasma levels, all 6 measurements were averaged and two-tailed T-test statistics was performed on this average (see Table I). Paroxetine-treated patients with at least one reduced activity CYP2D6 allele show significantly higher paroxetine levels ($P = 0.037$) compared to patients with normal alleles. Venlafaxine-treated patients with at least one reduced activity CYP2D6 allele show significantly higher venlafaxine levels ($P = 0.018$) compared to patients with normal alleles. When considering the venlafaxine metabolites, insignificant differences are found with lower *O*-desmethylvenlafaxine levels ($P = 0.397$) and higher combined venlafaxine + *O*-desmethylvenlafaxine levels ($P = 0.065$) compared to patients with normal alleles.

In patients with two reduced activity CYP2D6 alleles, the same results are found but with a higher statistical significance level. The plasma metabolite levels also differ significantly. Patients with two reduced activity CYP2D6 alleles show higher

Table I. Plasma levels and response in patients with at least one reduced activity CYP2D6 allele (poor metabolizers) versus patients with only normal alleles.

	Plasma levels (ng/ml)		Response (YBOCS decrease ≥25%)		Response (YBOCS decrease ≥35%)	
Paroxetine treated patients ($N = 35$)						
Poor metabolizer ($N = 17$)	177 ± 82	Two-tailed *t*-test $P = 0.037$	75%	χ^2-test df = 1 $P = 1.00$	55%	χ^2-test df = 1 $P = 1.00$
Normal metabolizer ($N = 18$)	125 ± 61		80%		50%	
Venlafaxine treated patients ($N = 39$)						
Poor metabolizer ($N = 22$)	390 ± 387	Two-tailed *t*-test $P = 0.018$	52%	χ^2-test df = 1 $P = 0.77$	44%	χ^2-test df = 1 $P = 0.76$
Normal metabolizer ($N = 17$)	151 ± 113		58%		53%	

Image 2

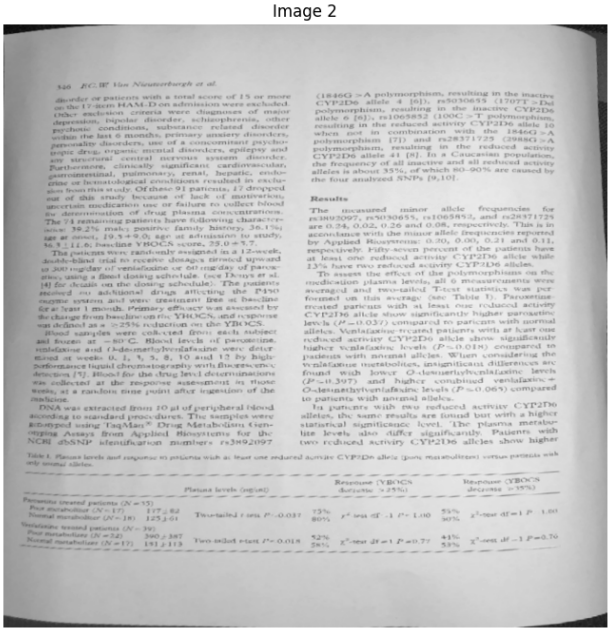

Figure 3: Correct Curved Example

Image 1

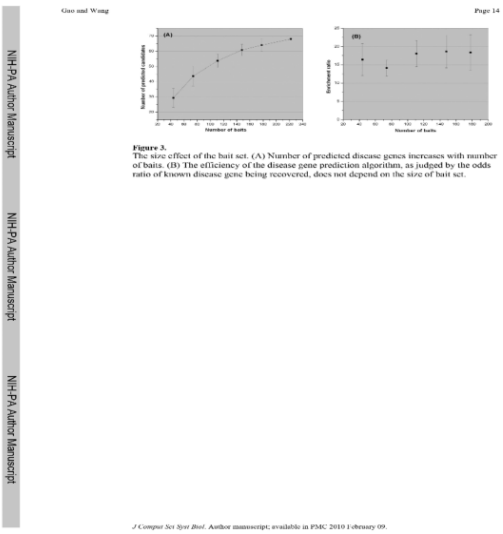

Image 2

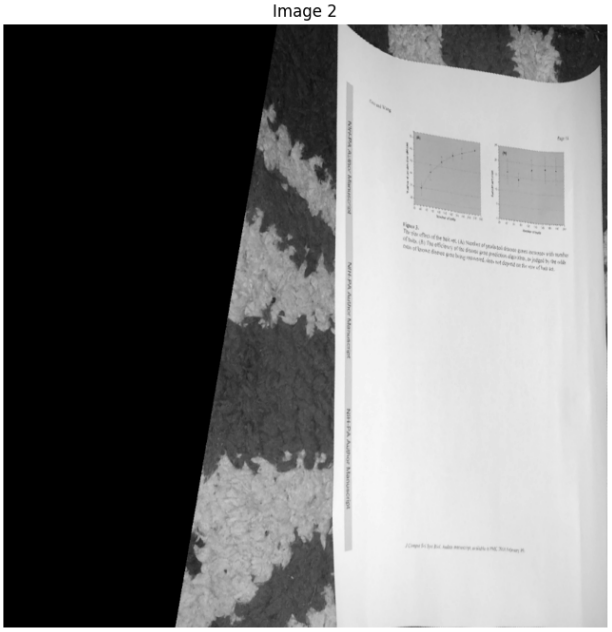

Figure 4: Incorrect Curved Example

Image 1

Image 2

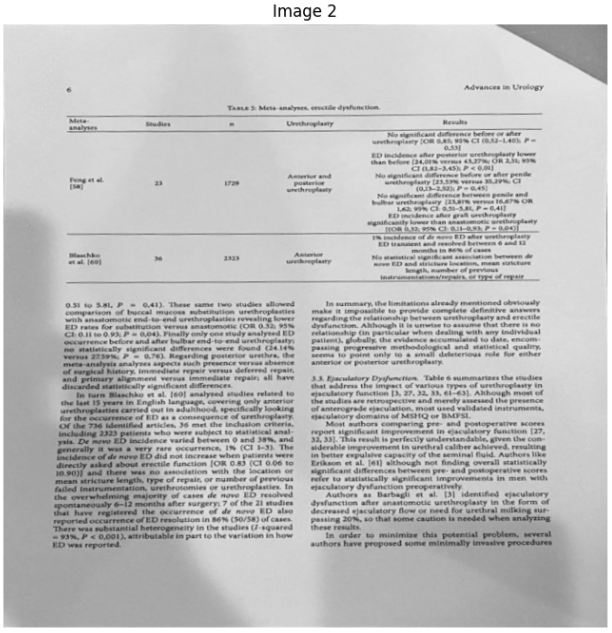

Figure 5: Correct Incomplete Example

Image 1

2 International Journal of Pediatrics

Moreover, children with epilepsy are at an increased risk for a number of education-related problems such as educational underachievement, learning disabilities, mental health problems, and social isolation. Sometimes, social attitude and discrimination against children with epilepsy are more devastating and harmful than the disease itself [5].

Knowledge about Epilepsy. Knowledge about epilepsy is an important issue in determining teachers' attitudes toward children with epilepsy. In general, teachers do not receive any formal instructions on epilepsy during their education and training despite the fact that as much as 40% of the children's developing life is spent at school [3]. In Kuwait, teachers are considered as social leaders and role models thus influencing the child's critical period of social and psychological development. For that reason, studying teachers' knowledge about epilepsy is beneficial for promoting our future generations.

Teachers' Attitudes toward Students with Epilepsy. Teachers' attitude toward epilepsy is their predisposition or tendency to respond positively or negatively toward various issues related to students with epilepsy. These attitudes influence their choice of action and responses to challenges, incentives, and rewards.

Although attitude is a complex and abstract construct, recent studies have demonstrated the manner in which teachers' attitudes may be translated into behaviors that can have problematic results for students with epilepsy. Teachers' perception of and approach to these students with epilepsy varies with the accuracy of their knowledge, which is often inadequate, limited, or even erroneous [6]. Kankirawatana [7] conducted a survey of 360 schools in Thailand in 1999 and reported that 15% of the respondents preferred to place all children with epilepsy in a special classroom. This preference may result from fear of handling the seizure of a student in the class. Furthermore, half of the respondents who had experience with first-aid management of seizures used improper and potentially harmful measures. Kankirawatana also concluded that, in addition to the proper management of epilepsy, there is a need for a general public education campaign about epilepsy to address and correct the existing biases. Such biases have been reported by some studies [3], which concluded that some teachers believe that epilepsy could be enough reason to prevent marriage or have children or could even be a justification for divorce. Also, it has been recognized that the mythical idea of epilepsy as a contagious disease seems to be one of the most relevant biases observed [8]. Furthermore, many teachers objected to the fact that persons with epilepsy can safely operate machinery and marry thought that other children need to be protected from them. A few even thought that laws barring epileptic children from being adopted should be applied [9].

Objectives. The objectives of our study were as follows:

(1) Evaluating middle and high school teachers' knowledge about epilepsy.

(2) Assessing teachers' attitudes toward students with epilepsy.

(3) Investigating the association of sociodemographic characteristics and teaching experience of teachers with their knowledge and attitudes.

2. Methods

2.1. Study Design and Participants. This cross sectional study was conducted during March 2013 in Kuwait. The target population was middle and high school teachers in the 6 governorates of Kuwait, namely, Capital, Hawalli, Al-Farwaniya, Al Ahmadi, Al Jahra, and Mubarak Al Kabeer. Twenty four schools (12 male and 12 female schools) were randomly selected from the sampling frame obtained from the Ministry of Education. The sampling method was multistage stratified cluster sampling. All available eligible teachers in selected schools during the data collection period were included in the study with schools as clusters. The total number of teachers who were approached was 850, of whom 824 accepted to participate. Hence, the response rate was 96.9%.

2.2. Ethical Considerations. An informed consent was obtained from each participant; and it clearly stated that participation in this study is optional and that there is no risk as a result of participation in the study. In order to ensure the confidentiality, names of participants or other identifying information was not obtained from the teachers. A Human Subject Form was completed, and the research was approved by the Department of Community Medicine Ethics Review Board and the Research Ethics Committee of Health Sciences Center, Kuwait University. Permission for conducting the research was obtained from the Ministry of Education and the administration of each selected school.

2.3. Data Collection Instrument and Procedures. Participants were asked to complete a self-administered questionnaire, comprising of 26 questions. The English version of the questionnaire was translated into Arabic using simple and clear words that would convey the same meaning as the English version. The Arabic version was back-translated into English by an independent bilingual person in order to ensure that the Arabic version provides the same meaning as the English one. The questionnaire was pretested by administrating it to 10 teachers, in order to emphasize that its items were clear and to estimate the time required to complete the questionnaire, which was found to be approximately 10 minutes. The study questionnaire was divided into 5 sections.

Section 1. Sociodemographic characteristics (Questions 1 to 6) included information about the respondents' age, gender, nationality, marital status, number of children, and highest level of education.

Section 2. Teaching experience (Questions 7 to 10) included questions about the level of school the teacher is working at, the respondents' position, how long he has been working as a teacher, and what subjects he teaches.

Section 3. Experience with epilepsy (Questions 11 to 24) included questions regarding persons with epilepsy and their

Image 2

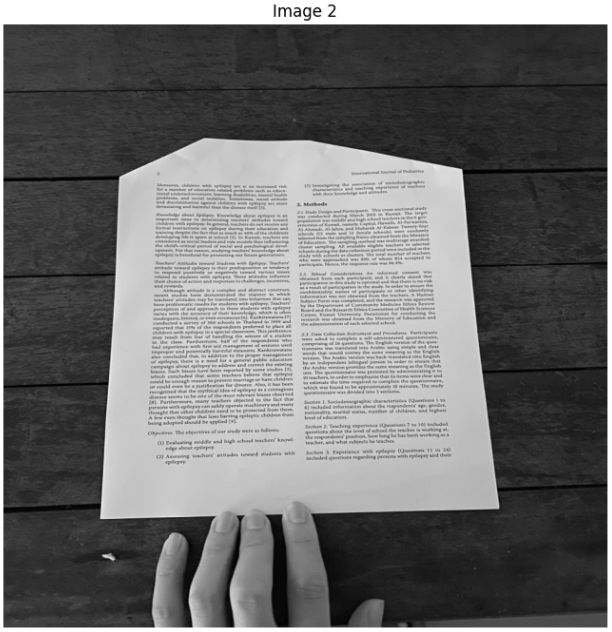

Figure 6: Incorrect Incomplete Example

Image 1

Computational and Mathematical Methods in Medicine 7

To compute the error, we considered all intensities of brain MR images. In other words, the estimated distribution and real image histogram should be compared at each intensity. The amount of error is the average difference between estimated distribution and original distribution at related intensity:

$$\text{Error} = \frac{1}{N}\sum_{i=1}^{m}(f_i - g_i), \tag{8}$$

where N is the number of intensities that consists of Gaussian distribution, f_i is the number of voxels in related intensity of real histogram, and g_i is the number of voxels in related intensity of estimated histogram. Consequently, in this section minimum error and optimum parameters are estimated. Finally, it is repeated two more times to provide the three distributions that best fit the histogram.

After the modified EM converges, the parameters that maximize the likelihood function are then applied to segment brain image into three tissue classes. In this step we compute the membership probability with the estimated parameters. The initial brain volume is updated by adding the voxels, which are labeled as brain regions (WM, GM, and CSF) based on the value of membership probability. The process continues by checking every neighboring voxel of an already labeled one, until the left and right brain volumes remain unaltered. The outermost voxels of corresponding unaltered brain volumes provide the final left and right brain borders. The coordinates of each labeled voxels are stored to avoid double checking of neighboring voxels during the brain volume updating.

The modified algorithm is summarized as follows.

(1) Choose the number of Gaussian distributions and separate them based on the gradient-based method.

(2) Select one Gaussian distribution in the split histogram.

(3) Parameter initialization is as follows.

E-step: estimate distribution over labels given a certain fixed model.

M-step: choose new parameters for model to maximize expected log-likelihood of observed data and hidden variables.

Outputs: these are μ_i and $\sigma_{\text{first-side}}$.

(4) Assume the following.

(a) The estimated mean is correct and the $\sigma 1$ is the standard deviation of one side.

(b) Standard deviation of the other side is $\sigma 2 = r \cdot \sigma 1$.

r changes 10 percent at each calculation.

The defined threshold determines when calculation should be stopped.

(5) Calculate error between the estimated distribution and real image histogram and obtain the optimal value of r.

If the error has reached threshold (an acceptable error that is defined in the first stage) then estimation is complete.

If error is more than threshold, estimation will be continued.

(6) Continue steps (4) and (5) until the convergence of the sequence of parameters is reached.

(7) Keep the estimated distribution and estimate the next separated distribution.

(8) Compute the membership probability with the estimated parameters.

(9) Assign each voxel to the Kth class.

However, because of the intensity similarity between GM and CSF or CSF and WM and overlapping problem in the brain MR images the next improvement stage is required to have powerful segmentation. To have a robust and accurate segmentation in the next step we will extract some textural features from the image and finally use SVM to improve the classification process.

2.8. Feature Extraction. The goal of feature extraction is to reduce the original dataset by extracting the most important features. Choosing the optimal features has a strong effect on classification results. Image intensities are the most prominent features for image segmentation. Using intensity information as the only features in MR image is not sufficient due to several reasons.

(i) In some scans, the nonbrain voxels have a similar intensity to GM, WM, and CSF.

(ii) The intensity of constructing brain tissues varies among different slices.

(iii) In some slices, the intensity of different tissues is similar.

Therefore, we carried out texture analysis for describing texture of the images to have adequate features for accurate segmentation. We also extracted useful features such as first- and second-order texture information in this study to have an appropriate segmentation for all cases.

In the previous section voxel labeling is initially applied on each voxel of the brain using intensity information with some new ideas. Since overlapped voxels (voxels of brain borders) have two labels (GM, CSF or GM, WM) instead of one, to compensate for this problem, the overlapped voxels should be classified to identify which classes they exactly belong to. Thus, in this section to have robust and accurate brain segmentation, each overlapped voxel and its 18-connected neighbors are used as input for 3D statistical features extraction technique, which is an improvement stage. In other words the input of 3D GLCM is the target area in the rectangular region of interest [33] that is demonstrated in Figure 6.

One of the important issues in the field of image analysis is the question of how to determine the texture differences of complex images. These differences are often due to

Image 2

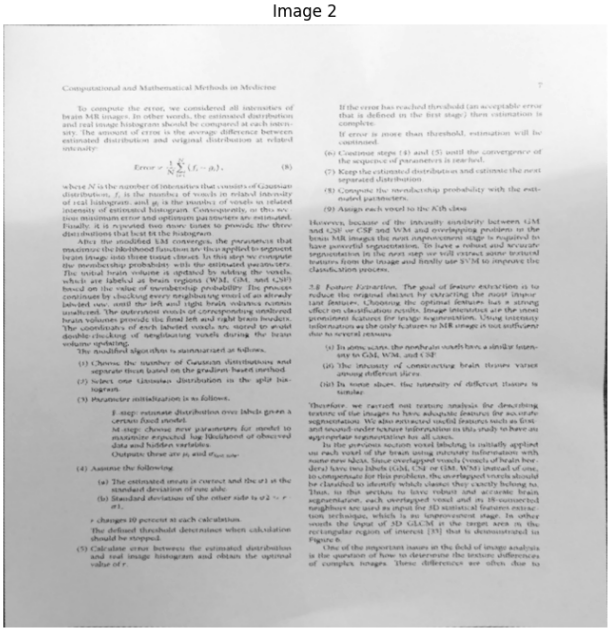

Figure 7: Correct Perspective Example

Image 1

Federica Paganelli et al. 11

Table 2: Mean and standard deviation values of alarm detection (T_{ALARM}), alert policy definition (T_{POLICY}) and management, and overall alarm management times ($T_{MANAGEMENT}$) in a basic Context Management configuration.

Alarm level	T_{ALARM}		T_{POLICY}		$T_{MANAGEMENT}$	
	Time slot 1	*Time slot 2*	*Time slot 1*	*Time slot 2*	*Time slot 1*	*Time slot 2*
	Average		*Average*		*Average*	
Very low	1367 ± 220	1338 ± 213	869 ± 203	843 ± 175	7728 ± 931	6814 ± 1303
	1419 ± 238		851 ± 186		6196 ± 1217	
Low	1457 ± 207	1360 ± 217	879 ± 218	869 ± 203	8235 ± 618	6963 ± 1247
	1409 ± 217		874 ± 210		760t ± 1168	
Medium	1455 ± 178	1576 ± 220	865 ± 215	869 ± 232	8433 ± 652	7837 ± 680
	1515 ± 208		867 ± 223		8137 ± 728	
High	1402 ± 201	1576 ± 222	859 ± 231	855 ± 225	7481 ± 610	8848 ± 635
	1489 ± 229		857 ± 222		8164 ± 925	

As mentioned above, this paragraph focuses on performance estimation of the Context Management system in delivering the most critical service (alarm detection and handling). Thus, our evaluation is based on measured values of T_{ALARM}, T_{TRANSM}, and T_{POLICY}. Values of further parameters (T_{TRANSM}; T_{MHIM}, T_{IMS} and T_{IM}) are not available for dissemination as they have been collected by the industrial partner (HP, Italy). Moreover, values of T_{IMS} and T_{IM} are dependent on the characteristics of the network infrastructure. In a real implementation scenario, these parameters might be optimized according to appropriate technological choices, such as using public or professional radio-mobile networks for SMS delivery (i.e., GSM and TETRA, resp.) and a dedicated fixed line for communicating with the emergency operators, as well as establishing proper service level agreements with network operators.

To estimate the performance of the implemented system in detecting and managing alarms, we have simulated the generation of 60 sample alarms for each of the four alarm levels ("Very low," "Low," "Medium," and "High"). Such samples have been acquired by monitoring the activity of the Context Management system upon an interval of five working days, during working hours, in order to stress the system during worst traffic conditions (i.e., peak traffic hours). In more detail, experiments were performed during two time slots: 10:00 A.M.–2:00 P.M. (*Time Slot 1*) and 2:00 P.M.–6:00 P.M. (*Time Slot 2*).

Table 2 reports the mean and standard deviation values in milliseconds of alarm detection time (T_{ALARM}), alert policy time (T_{POLICY}), and the overall alarm management time ($T_{MANAGEMENT}$), which is calculated as the sum of T_{ALARM}, T_{POLICY}, and the transmission delay (T_{TRANSM}).

Measured values of T_{ALARM} as well as T_{POLICY} do not vary significantly across alarm level. T_{POLICY} measured values are higher than T_{ALARM} ones as the major part of the processing load is leaning to the PatientCM side, according to the architecture of the Context Managers.

Measured values of the overall $T_{MANAGEMENT}$ vary significantly according to network traffic conditions which directly influence T_{TRANSM} values. In this experiment, we can estimate an overall alarm time swinging between 8 and 10 seconds, with a transmission delay that can be evaluated in about 5 seconds. The higher values of the standard deviation for alarm times can be charged on interferences in the PatientCM wireless connection and on the network conditions in the restricted observation window (five working days) considered for this evaluation.

We expect that a more performant connection would significantly improve the Alarm Management Time, and a wider observation interval (i.e., one month) would produce more uniform statistics for this indicator.

In order to minimize reasoning tasks execution time (inference on ontology instances), we perform reasoning on small ontologies populated by a small number of instances, since ontological reasoning execution times grow at least linearly with respect to the ontology size [26]. This time could be further optimized by performing part of the reasoning task before the service request. Future research activities will thus focus on analyzing which reasoning tasks could be performed prior to service requests and consequently on reengineering the PatientCM and CentralCM.

5.2. User trials

As ERMHAN services have been designed to support care networks and thus to address requirements of care providers, testing is primarily to be focused on evaluating health operators' acceptance of implemented features.

A trial has been performed in a nursing home in Piacenza for system evaluation by profesional caregivers. Further trials are planned in a nursing home in Florence in the near future, for more extensive evaluations by chronic condition patients. For these future tests, a sensing system for vital signs and environmental monitoring will also be deployed. Testing activities will thus focus also on evaluating patient acceptance with regard to deployed services (i.e., monitoring, medicine reminder, help, and communication request services).

In the testing stage already conducted in Piacenza, biomedical and environmental sensing was simulated by a web application. Biomedical parameters that were represented in the model included heart rate frequency, pulse

Image 2

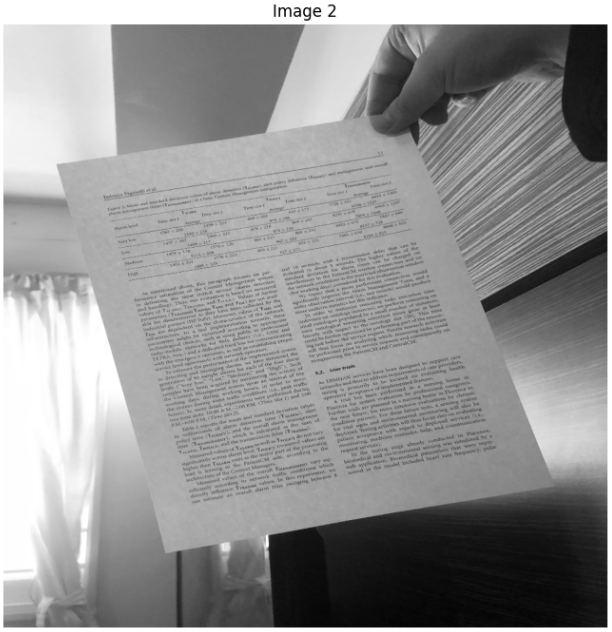

Figure 8: Incorrect Perspective Example

Image 1

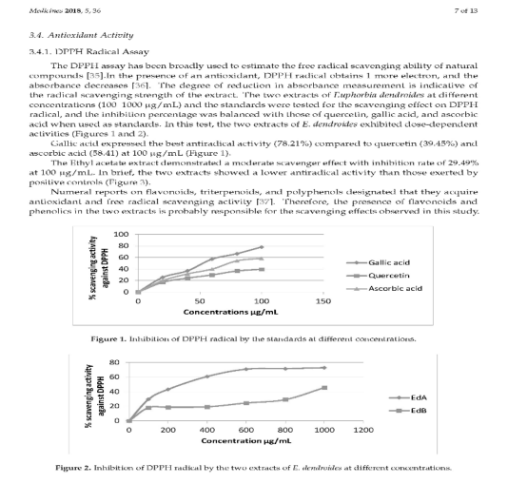

Medicines **2018**, *5*, 36 7 of 13

3.4. Antioxidant Activity

3.4.1. DPPH Radical Assay

The DPPH assay has been broadly used to estimate the free radical scavenging ability of natural compounds [35].In the presence of an antioxidant, DPPH radical obtains 1 more electron, and the absorbance decreases [36]. The degree of reduction in absorbance measurement is indicative of the radical scavenging strength of the extract. The two extracts of *Euphorbia dendroides* at different concentrations (100–1000 µg/mL) and the standards were tested for the scavenging effect on DPPH radical, and the inhibition percentage was balanced with those of quercetin, gallic acid, and ascorbic acid when used as standards. In this test, the two extracts of *E. dendroides* exhibited dose-dependent activities (Figures 1 and 2).

Gallic acid expressed the best antiradical activity (78.21%) compared to quercetin (39.45%) and ascorbic acid (58.41) at 100 µg/mL (Figure 1).

The Ethyl acetate extract demonstrated a moderate scavenger effect with inhibition rate of 29.49% at 100 µg/mL. In brief, the two extracts showed a lower antiradical activity than those exerted by positive controls (Figure 3).

Numeral reports on flavonoids, triterpenoids, and polyphenols designated that they acquire antioxidant and free radical scavenging activity [37]. Therefore, the presence of flavonoids and phenolics in the two extracts is probably responsible for the scavenging effects observed in this study.

Figure 1. Inhibition of DPPH radical by the standards at different concentrations.

Figure 2. Inhibition of DPPH radical by the two extracts of *E. denbroides* at different concentrations.

Image 2

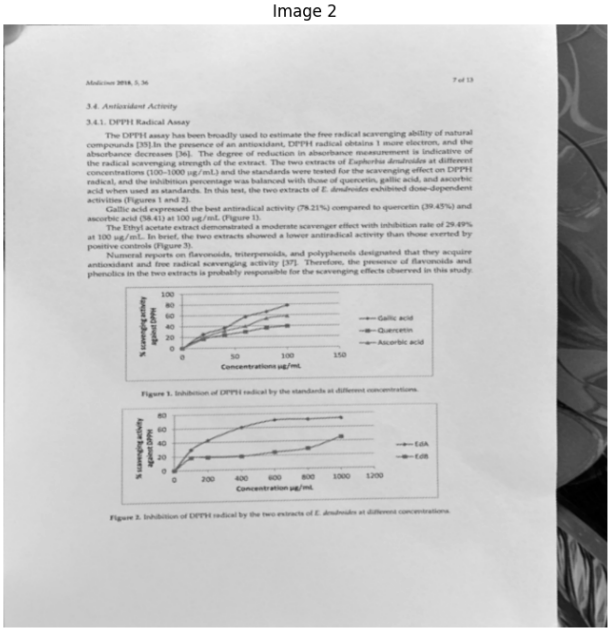

Figure 9: Correct Rotate Example

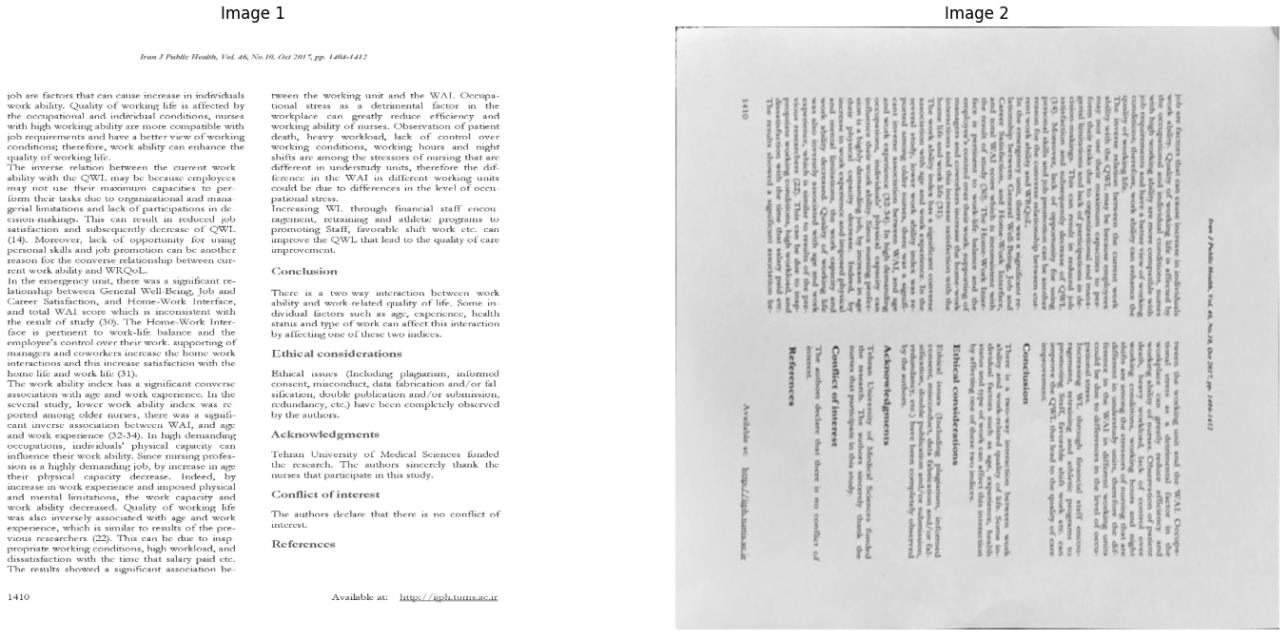

Figure 10: Incorrect Rotate Example

Comments

Looking at the examples, the algorithm has a few fundamental error causes. First, inadequate line detection can result in failure to find the appropriate rectangle, as seen in Figure 2 and Figure 4. Additionally, the presence of rectangular structures within the image can cause the algorithm to detect an excessively large rectangle, as demonstrated in Figure 6. Another common issue is the inability to apply the transformation due to insufficient lines to form a rectangle, as observed in Figure 8. Finally, even when the paper is correctly detected, the algorithm may apply the warp in the wrong direction, as seen in Figure 10.

Results

	*C*urved	Fold	Incomplete	Perspective	Random
	*0.*20276961879593677	0.20094835407299386	0.21946030064507657	0.2202182650132417	0.20564519723268673

Table 1: Results from experiments.

There are several reasons why there is only one test result in the table. I conducted many tests with the current algorithm that were not fully completed, but I did not record them because the SSIM values were too low. Ultimately, I performed and recorded this test because I considered these values to be normal for this dataset. Additionally, I could not conduct further tests due to the significant increase in processing time caused by changes in certain parameters.

Final Comments

Looking at the results, we can see that the SSIM values are indeed very low. Even in tests performed on images where the transformation was applied perfectly, I observed SSIM values below 0.4. Therefore, even if all images are processed correctly, it does not seem likely for the SSIM values to exceed 0.6. Similarly, the downscaling of images to 1024x1024 pixels for performance improvement also lowered the SSIM values. As I mentioned in the Quadrilateral Detection section, if we had processed the images less and preserved their original states for testing, the SSIM values could have been higher. However, in such a case, we would have achieved nothing toward our ultimate goal. While the current algorithm provides a good foundation, I believe it can be significantly improved by fine-tuning the parameters.